3D Free-Standing Graphene: Influence of Etching Solution and Etching Time on Chemical Vapor Deposition on the Graphene/Nickel Foam

Nurul Nabila Rosman[a], Rozan Mohamad Yunus[a]*, Nur Rabiatul Adawiyah Mohd Shah[a], Khuzaimah Arifin[a], Lorna Jeffery Minggu[a] &
Norasikin Ahmad Ludin[b]

[a] *Fuel Cell Institute, Universiti Kebangsaan Malaysia, 43600 UKM Bangi, Selangor, Malaysia*
[b] *Solar Energy Research Institute, Universiti Kebangsaan Malaysia, 43600 UKM Bangi, Selangor, Malaysia*

*Corresponding author: rozanyunus@ukm.edu.my

ABSTRACT

Three-dimensional (3D) structures made of graphene sheets have been developed recently, and have resulted in the development of a new class of graphene materials known as 3D graphene materials. High-quality free-standing 3D graphene foam has been synthesized by chemical vapor deposition (CVD) on nickel foam followed by a chemical etching process to remove the nickel foam as a template. Field-emission scanning electron microscopy (FESEM), x-ray diffraction (XRD), and Raman spectroscopy measurements were performed to investigate the morphologies, crystal phase, and the structure of nickel foam (NF), graphene/nickel foam (Gr/NF), and 3D graphene (3D Gr). In this study, the influence of etching solution and etching time on Gr/NF to produce free-standing 3D Gr was investigated. XRD spectroscopy showed that the mixed solutions of 1M FeCl$_3$:1M HCl at 80 °C for 3 h can significantly remove the NF and no peaks of NF are observed, thus indicating a high crystal quality of 3D Gr was obtained. In addition, XRD spectroscopy revealed that by increasing the etching time beyond 3 h, the intensity of diffraction peaks decreases, thus degrading graphene quality. This research emphasizes the significance of proper selections of etching solution and etching time in removing the NF to maintain the characteristic, quality, and surface morphology of 3D Gr after the etching process.

Keywords: 3D graphene; chemical vapor deposition; etching solution; etching time

INTRODUCTION

Graphene has a lot of potential usage in various applications including energy storage, optoelectronics, and electronics owing to its extraordinary properties (Ibrahim et al. 2017). Two-dimensional (2D) graphene subsequently received great focus and exploration because of its excellent electrical and thermal conductivity, outstanding mechanical stability, cycle flexibility, and theoretically high specific surface area of (2630 m^2 g^{-1}) (Othman & Zainordin 2021; Rosman et al. 2018; Wang et al. 2019). However, there are some difficulties in optimizing the 2D graphene such as the graphene sheets tend to stack or aggregate together leading to the limitation of the ion transfer, electron transport, and gas product dispersion caused by the existing strong van der Waals force and π–π interactions (Kuang et al. 2020). Therefore, 3D graphene network development can be a solution as the restacking and aggregation of the adjacent layers are greatly reduced. 3D graphene has the special characteristics of graphene nanosheets, and it also has several advantages, including a very low mass density, high specific surface area, interconnected and hierarchical structure, and outstanding mechanical stability (Chen et al. 2018; Kuang et al. 2020; Mohd Shah et al. 2021). The

superior properties of these 3D graphene constructions make them useful in various applications, such as solar cells, catalysis, supercapacitors, sensors, batteries, environmental decontaminations, conductors, and so on (Chen et al. 2011; Sun, Fang & Hu 2020).

Various methods were used to produce high-quality graphene, which is necessary to fully utilize its specific electrochemical, structural, and thermal characteristics, thus contributing to a diverse range of high-performance applications. Given the low number of graphene defects, great uniformity, and easy to scale up, the chemical vapor deposition (CVD) approach has been widely used to grow large areas of graphene on nickel foam (NF) template, thus exhibiting superior electrochemical efficiency to chemically prepared graphene (Barin et al. 2015; Lee et al. 2017). However, etching of the CVD graphene from NF is still an extremely difficult and crucial procedure. For example, Chen et al. successfully produced 3D graphene (3D Gr) foam by etching the nickel substrate using an etching solution and removing the polymethyl methacrylate (PMMA) layer in acetone. The PMMA is necessary for the formation of the free-standing, scalable, and interconnected 3D Gr network (Chen et al. 2011; Kuang et al. 2020). Nevertheless, contaminants are incorporated into the generated 3D graphene in this

way, and several modifications in the surface morphology of pristine 3D graphene can be recreated if the PMMA remained on it (Sun, Fang & Hu 2020). The 2D intensity is reduced from the Raman spectrum by the PMMA residues present on the graphene surface. This is caused by the PMMA residues present on the graphene surface creating the p-type doping effect (Son et al. 2017). The effect of chemical etching of graphene growth on copper (Cu) foil has been studied, and the results showed that in a short period, Cu etching produced a smooth surface with few and small etch pits by using ammonium persulfate as the etching solution (Ibrahim et al. 2017). However, Cu residues on the graphene surface resulted from an incomplete Cu etching time. Some commercially available Cu etching solutions are ineffective at entirely removing Cu residues (Deokar et al. 2015). Thus, determining the best etching solution is required to completely remove the template to produce a free-standing 3D graphene foam.

In this paper, the influence of each parameter on the chemical etching technique is reported. An evaluation of how the etching solution affects the results have been discussed in detail. The effect of etching time and temperature of PMMA/Gr/NF in etching solution to completely remove the NF on the graphene contact was also studied. This research aims to reveal the effect of each step of the chemical etching process on the properties, structure, and morphology of graphene, hence suggesting an optimization of the graphene etching process.

METHODOLOGY

GRAPHENE GROWTH

Graphene was grown on NF (purchased from TOB) using the CVD method. Prior to graphene growth, the NF was thoroughly cleaned in acetone, ethanol, and deionized water for 10 min each to remove impurities and dried by a nitrogen (N_2) blower before being loaded into the quartz tube. The first step, the NF substrate was purged with Argon (Ar) flow, followed by ramping up the furnace temperature up to 1000 °C under Ar (100 sccm) and hydrogen (H_2) (400 sccm) at the rate of 20 °C. After the temperature reached 1000 °C, the Ar and H_2 were maintained for 50 min to clean the NF surface and eliminate a thin surface oxide layer. The growth step was carried out with the flow of methane (20 sccm), H_2 (250 sccm), and Ar (150 sccm) for 30 min at the same temperature. Finally, the chamber was cooled down to room temperature with the 500 sccm flow of Ar.

THE ETCHING PROCESS OF 3D GRAPHENE

Graphene was etched using the chemical etching method. The PMMA solution was spin-coated on the graphene/nickel foam at 1000 rpm for 30 sec. After coating, the sample was heated at 110 °C for 30 min. To etch the nickel foam, the PMMA/Gr/NF was soaked in different nickel etching solutions to study its effectiveness in removing the nickel template. The etching solutions that were used are:
1. 1 M $FeCl_3$ at room temperature for 24 h
2. 1 M HCl at room temperature for 24 h
3. 1 M $FeCl_3$:1M HCl at room temperature for 24 h
4. 1M $FeCl_3$ at 80 °C for 3 h
5. 1 M HCl at 80 °C for 3 h
6. 1M $FeCl_3$:1M HCl at 80 °C for 3 h

The suspended foam was transferred to deionized water for 30 min at 80 °C to remove any residual after the nickel etching. Subsequently, the PMMA layer was removed by soaking it in hot acetone for 3 h at 60 °C.

ETCHING TIME

Prior to this step, how the etching solution was made is explained in section "Etching process of 3D graphene", using 1M $FeCl_3$:1M HCl at 80 °C. The following changes were conducted to investigate the influence of each etching time:
1. 1 h at 80 °C
2. 2 h at 80 °C
3. 3 h at 80 °C
4. 4 h at 80 °C

STRUCTURAL CHARACTERIZATION

To confirm the presence of graphene, Raman spectroscopy (DXR2xi, Thermo Scientific) was performed on the samples. Field-emission scanning electron microscopy (FESEM, Zeiss AM10) was carried out in determining the surface morphologies of the samples. Finally, x-ray diffraction (XRD, D8 Advance) was utilized in determining the crystallographic structure of a material.
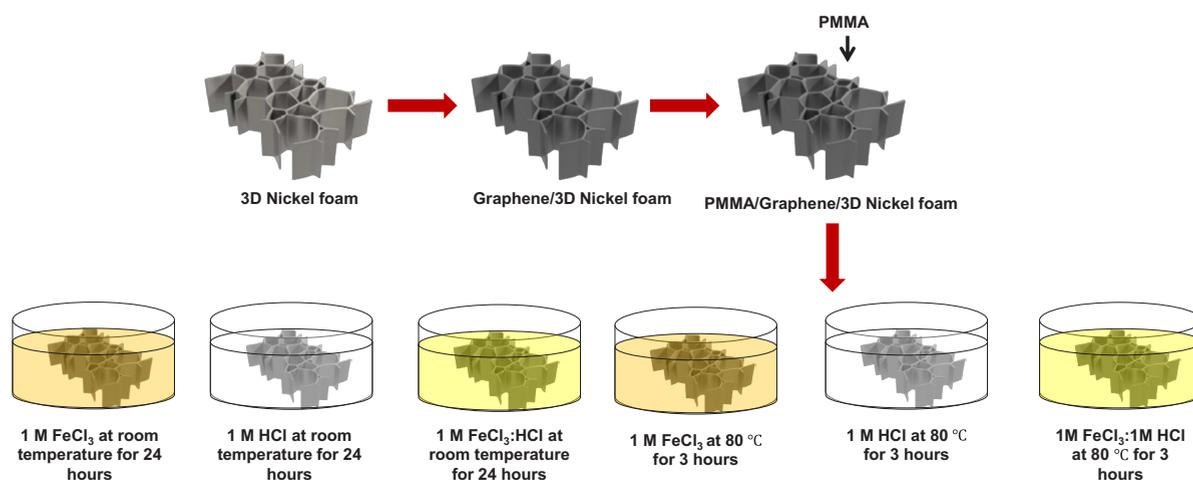
FIGURE 1. Schematic diagram of 3D graphene etching by chemical etching process

RESULTS AND DISCUSSION

Figure 1 shows the schematic diagram summarizing the fabrication of graphene grown on NF and the chemical etching process. Using the CVD method, graphene was deposited on the NF and then the NF were etched away with different etching solutions. Different etching solutions and etching times were used in obtaining a 3D and free-standing graphene foam without any nickel residues as explained in the methodology section. Figure 2 shows the FESEM morphologies of NF, Gr/NF, and 3D Gr. The NF was used as a template for the direct growth of graphene by promoting its lateral growth and lowering the energy barrier (Lee et al. 2017). The NF has a 3D structure, linear grain boundaries, and a smooth surface(Lee et al. 2017). The color of the NF turned from bright white (Figure 2[a-c]) to dark grey (Figure 2[d–f]) after an observable graphene growth. A 3D, transparent, and hollow graphene microtube structure (Figure 2[g–i]) was obtained by etching the nickel away using 1 M $FeCl_3$: 1 M HCl solution at 80 within 3 h. No existence of NF was noted after the etching process, which was further verified in Figure 3.
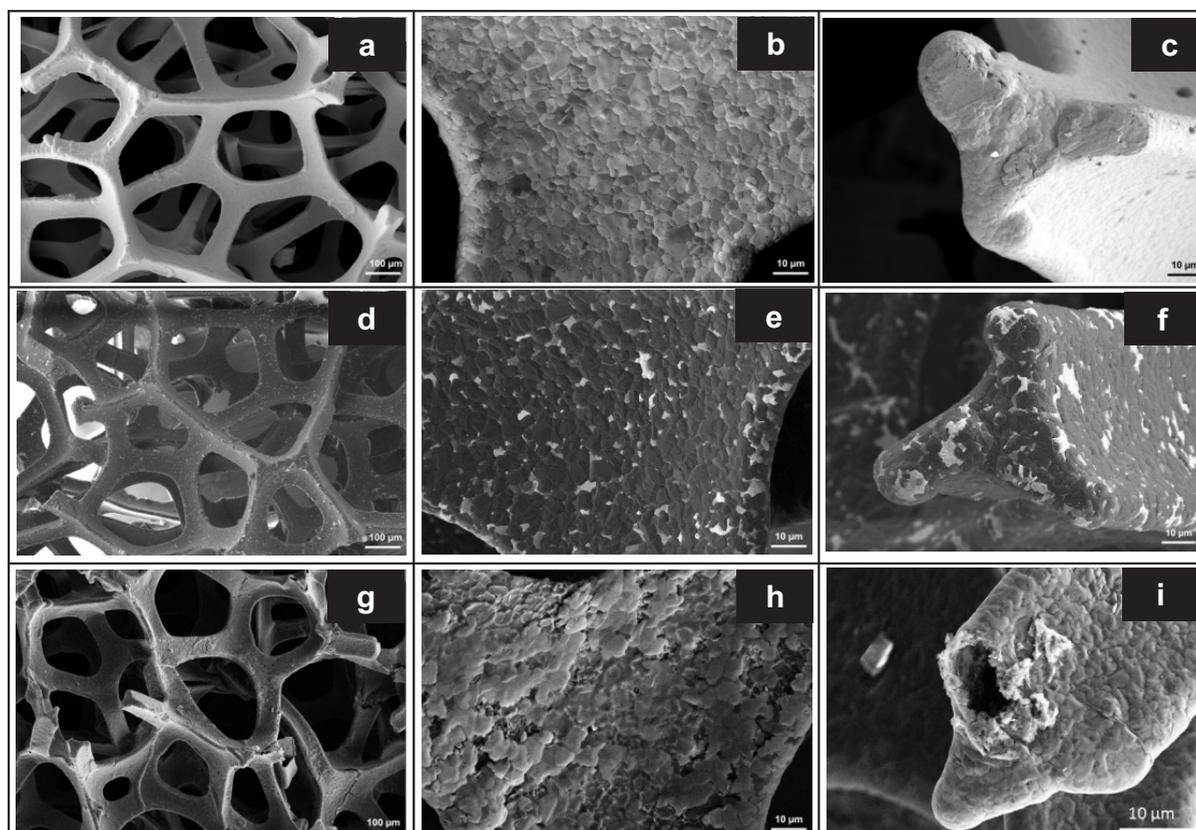
FIGURE 2. FESEM images of (a–c) 3D NF, (d–f) Gr/NF, and (g–i) 3D Gr after nickel was etched away

The XRD patterns of NF, Gr/NF, and Gr/NF were soaked in different etching solutions to remove the the NF are shown in Figure 3. The NF has a sharp peak centered at 2θ=44.5°, 51.8°, and 76.4° which can be indexed to the (111), (200), and (220) crystal planes of cubic nickel metal (JCPDS card No. 04-0850), respectively (Figure 3a) (Yan et al. 2020; Zhu et al. 2018). The Gr/NF (Figure 3b) showed another diffraction peak at 2θ=26.4, which corresponds to the (002) reflection of graphitic carbon (JCPDS card 75-1621). (Figure 3 [c–h]) show the samples soaked in the different etching solution at different temperature and time. The etching solutions used for samples in Figures 3 (c–e) and 3 (f–h) were 1 M FeCl$_3$, 1 M HCl, and the mixture of 1 M FeCl$_3$: 1M HCl at room temperature for 24 h at 80 °C for 3 h, respectively. All of the samples showed diffraction peaks of graphitic carbon at 26.4° and 54.6° which correspond to (002) and (004), respectively (Yue et al. 2017). However, nickel peaks still appeared in all the samples except in 1 M FeCl$_3$: 1M HCl etching solution (Figure 3e and 3h). Compared to the sample in Figure 3e, Figure 3h exhibits high-intensity diffraction peaks of graphitic carbon and revealed the high crystalline structure produced by the 3D Gr. Therefore, the best etching solution (1 M FeCl$_3$: 1M HCl) at 80 °C for 3 h can completely remove the nickel template from this study, because it was high as shown in the graphitic carbon peak and no Ni peak was detected in the sample. In addition, temperature also plays an important role in accelerating the etching rate. At high temperatures, an increase in molecular momentum can result in an increased etch depth (Patil & Mudigonda 2016).
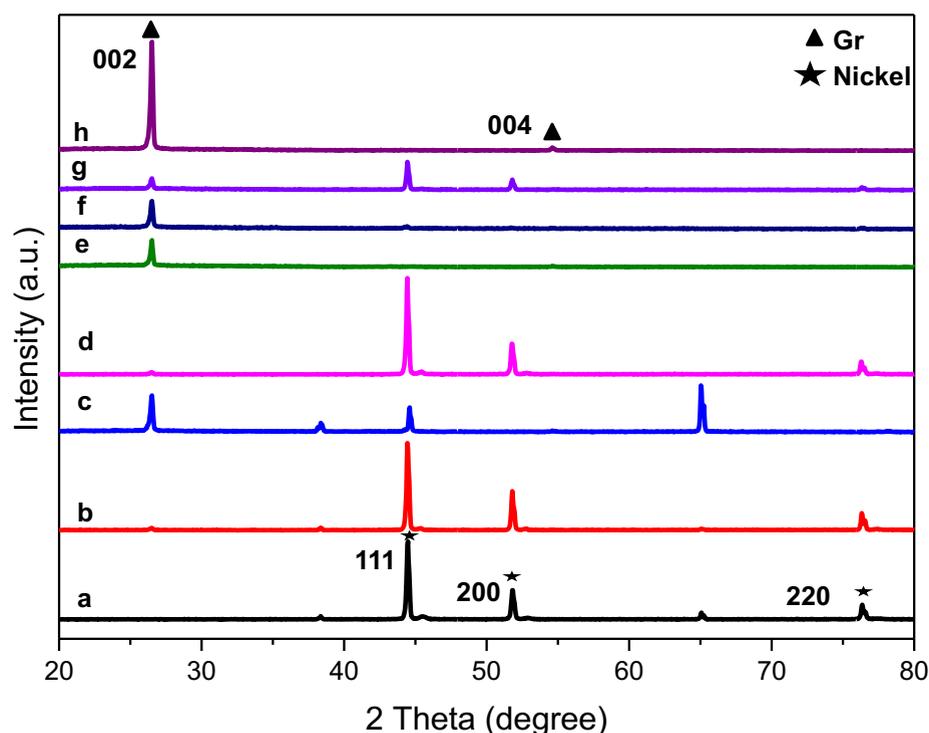
FIGURE 3. XRD pattern of (a) NF, (b) Gr/NF, (c) 3D Gr (1 M FeCl$_3$, room temperature, 24 H), (d) 3D Gr (1 M HCl, room temperature, 24 H), (e) 3D Gr (1 M FeCl$_3$: 1 M HCl, room temperature, 24 H), (f) 3D Gr (1 M FeCl$_3$, 80°C, 3 H), (g) 3D Gr (1 M HCl, 80°C, 3 H), and (h) 3D Gr (1 M FeCl$_3$: 1 M HCl, 80°C, 3 H)

Another XRD analysis was performed to study the influence of soaking time and its effect on completely removing the NF template for free-standing 3D Gr production by using the best etching solution (1 M FeCl$_3$:1 M HCl) at 80 for 3 h (Figure 4). The XRD patterns of all samples (1–4 h) show two diffraction peaks at 2θ=26.4° and 54.6°, which are attributed to the (002) and (004) reflections of graphitic carbon, respectively. No additional diffraction peaks were observed, indicating a high crystal quality of 3D GF was produced and the NF was completely etched away. The intensity of diffraction peaks of 3D Gr showed an increment of time from 1 h to 3 h. However, a further increase of the sample's soaking time in the solution resulted in a decreased intensity of diffraction peaks. It can be considered that the further increase in soaking time can degrade graphene quality. Thus, the results revealed that 3 h is the maximum soaking time to ensure a smooth and good quality free-standing 3D Gr surface.
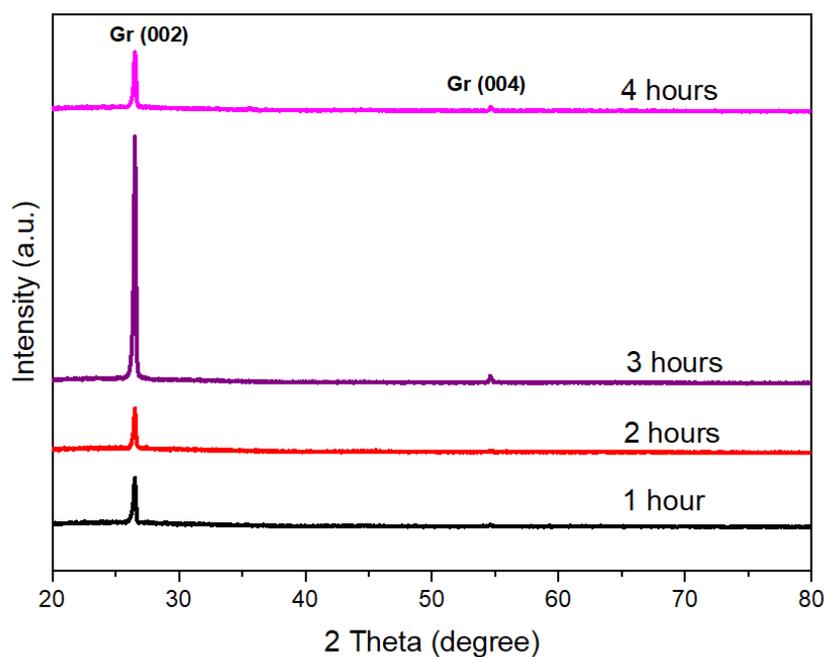
FIGURE 4. XRD of 3D Gr using 1 M FeCl$_3$: 1 M HCl etching solution at 80°C for 1–4 h

The Raman spectroscopy of NF, Gr/NF, and 3D Gr are shown in Figure 5. The Gr/NF and 3D Gr spectra show the characteristics of 2D and G bands at 2720 cm^{-1} and 1580 cm^{-1}, respectively (Rosman et al. 2020; Zhu et al. 2018). No appreciable D band intensity (~1350 cm^{-1}) is detected in both samples, thus indicating the high quality of graphene produced. The intensity ratio of 2D and G band (I_{2D}/I_G) of Gr/NF (0.40) and 3D Gr (0.46) indicated that both samples of graphene are multilayered (Shao et al. 2015).
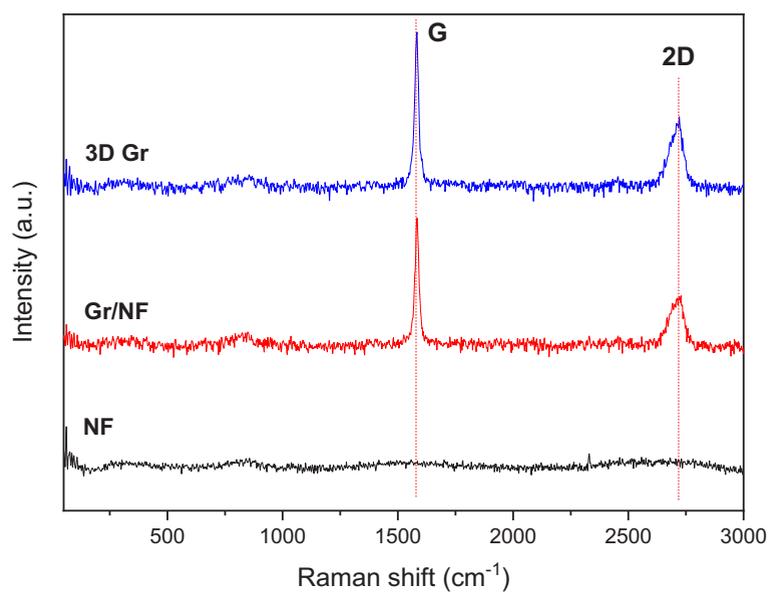
FIGURE 5. Raman specta of NF, Gr/NF, and 3D Gr

236

CONCLUSION

Free-standing 3D Gr from the chemical etching process by etching the NF from the CVD grown GR/NF was successfully prepared. FESEM, XRD, and Raman spectroscopy were performed to determine the influence of etching solution and etching time in producing high-quality free-standing 3D Gr. It was concluded that the mix solutions of 1 M FeCl$_3$: 1 M HCl could efficiently remove the NF template and other surface impurities at 80 within 3 h. The results in this work were believed to bring new insights in utilizing the 3D Gr in various applications given its unique network structure, high specific surface area, and remarkable electrical and mechanical capabilities.

DECLARATION OF COMPETING INTEREST

None

REFERENCES

Barin, G.B., Song, Y., Gimenez, I.D.F., Filho, A.G.S., Barreto, L.S. & Kong, J. 2015. Optimized graphene transfer: Influence of polymethylmethacrylate (PMMA) layer concentration and baking time on grapheme final performance. *Carbon* 84(C): 82–90.

Chen, K., Shi, L., Zhang, Y. & Liu, Z. 2018. Scalable chemical-vapour-deposition growth of three-dimensional graphene materials towards energy-related applications. *Chemical Society Reviews* 47(9): 3018–3036.

Chen, Z., Ren, W., Gao, L., Liu, B., Pei, S. & Cheng, H.M. 2011. Three-dimensional flexible and conductive interconnected graphene networks grown by chemical vapour deposition. *Nature Materials* 10(6): 424–428.

Deokar, G., Avila, J., Razado-Colambo, I., Codron, J.L., Boyaval, C., Galopin, E., Asensio, M.C. & Vignaud, D. 2015. Towards high quality CVD graphene growth and transfer. *Carbon* 89: 82–92.

Ibrahim, A., Nadhreen, G., Akhtar, S., Kafiah, F.M. & Laoui, T. 2017. Study of the impact of chemical etching on Cu surface morphology, graphene growth and transfer on SiO$_2$/Si substrate. *Carbon* 123: 402–414.

Kuang, P., Sayed, M., Fan, J., Cheng, B. & Yu, J. %J A.E.M. 2020. 3D Graphene-Based H$_2$-Production Photocatalyst and Electrocatalyst. *Advanced Energy Materials* 10(14): 1903802.

Lee, K., Lee, J., Kwon, K.W., Park, M.S., Hwang, J.H. & Kim, K.J. 2017. 3D Graphene-Ni Foam as an Advanced Electrode for High-Performance Nonaqueous Redox Flow Batteries. *ACS Applied Materials and Interfaces* 9(27): 22502–22508.

Mohd Shah, N.R.A., Mohamad Yunus, R., Rosman, N.N., Wong, W.Y., Arifin, K. & Jeffery Minggu, L. 2021. Current progress on 3D graphene-based photocatalysts: From synthesis to photocatalytic hydrogen production. *International Journal of Hydrogen Energy* 46(14): 9324–9340.

Othman, R.N. & Zainordin, M.S. 2021. Thermal conductivity properties of graphene based epoxy nanocomposite (Sifat Kekonduksian termal nanokomposit epoksi berasaskan grafin). *Jurnal Kejuruteraan* 4(2): 59–64.

Patil, D.H. & Mudigonda, S. 2016. The effect of the rolling direction, temperature, and etching time on the photochemical machining of Monel 400 Microchannels. *Advances in Materials Science and Engineering* 2016: 6751305.

Rosman, N.N., Mohamad Yunus, R., Mohamed, M.A., Arifin, K., Jeffery Minggu, L., Kassim, M.B. & Salehmin, M.N.I. 2018. Photocatalytic properties of two-dimensional graphene and layered transition-metal dichalcogenides based photocatalyst for photoelectrochemical hydrogen generation: An overview. *International Journal of Hydrogen Energy* 43(41): 18925–18945.

Rosman, N.N., Yunus, R.M., Minggu, L.J., Arifin, K., Kassim, M.B. & Mohamed, M.A. 2020. Vertical MoS$_2$ on SiO$_2$/Si and graphene: effect of surface morphology on photoelectrochemical properties. *Nanotechnology* 32(3): 35705.

Shao, D., Gao, J., Xin, G., Wang, Y., Li, L., Shi, J., Lian, J., Koratkar, N. & Sawyer, S. 2015. Cl-Doped ZnO Nanowire arrays on 3D graphene foam with highly efficient field emission and photocatalytic properties. *Small* 11(36): 4785–4792.

Son, B.H., Kim, H.S., Jeong, H., Park, J.Y., Lee, S. & Ahn, Y.H. 2017. Electron beam induced removal of PMMA layer used for graphene transfer. *Scientific Reports 2017 7:1* 7(1): 1–7.

Sun, Z., Fang, S. & Hu, Y.H. 2020. 3D Graphene Materials: From understanding to design and synthesis control. *Chemical Reviews* 120(18): 10336–10453.

Wang, Y., Zhang, W., Guo, X., Jin, K., Chen, Z., Liu, Y., Yin, L., Li, L., Yin, K., Sun, L. & Zhao, Y. 2019. Ni-Co Selenide Nanosheet/3D Graphene/Nickel Foam Binder-Free Electrode for High-Performance Supercapacitor. *ACS Applied Materials and Interfaces* 11(8): 7946–7953.

Yan, J., Huang, Y., Zhang, L., Zhou, M., Yang, P., Chen, W., Deng, X. & Yang, H. 2020. Preparation of MoS$_2$-Graphene-NiO@Ni foam composite by sol coating for (photo)electrocatalytic hydrogen evolution reaction. *Journal of Sol-Gel Science and Technology* 93(2): 462–470.

Yue, H.Y., Zhang, H., Huang, S., Lin, X.Y., Gao, X., Chang, J., Yao, L.H. & Guo, E.J. 2017. Synthesis of ZnO nanowire arrays/3D graphene foam and application for determination of levodopa in the presence of uric acid. *Biosensors and Bioelectronics* 89: 592–597.

Zhu, L., Guo, X., Liu, Y., Chen, Z., Zhang, W., Yin, K., Li, L., Zhang, Y., Wang, Z., Sun, L. & Zhao, Y. 2018. High-performance Cu nanoparticles/three-dimensional graphene/Ni foam hybrid for catalytic and sensing applications. *Nanotechnology* 29(14): 145703.